The Ionospheric Effects Symposium 2023

Abstract Book

Global Responses of Equatorial/Low-Latitude Ionosphere to CME-driven and CIR-driven Geomagnetic Storms

Akala, Andrew *University of Lagos*

Storm-time hourly morphologies of the Equatorial Ionization Anomaly (EIA) crests and their extended features along 110–125oE meridian

Akala, Andrew   *University of Lagos*

Ayangbemi, John A., Department of Physics, University of Lagos, Nigeria

Otsuka, Yuichi, Institute for Space-Earth Environment, Nagoya University, Nagoya, Aichi, Japan

This study investigates storm-time hourly morphologies of the Equatorial Ionization Anomaly (EIA) crests and their extended features along the Asian/Australian meridian lines. We used TEC derived from the observation data obtained from GPS receivers lined at ~±75o latitude along 110-125oE meridian. Four geomagnetic storms of 2013 and 2015 St. Patrick's Days, 1 June 2013, and 7 October 2015 were studied. The quiet days of the month of each storm occurrence was used as reference to evaluate storm-time responses of the EIA-TEC to geomagnetic storms. There were clear hemispheric asymmetries in plasma distributions. At 0000–0500 LT, plasma was localized around the magnetic equator with a single peak for each hour. At 0600–1100 LT, bifurcation of the EIA peaks gradually commenced, with both peaks tilted to the northern hemisphere but the southern crest recorded higher magnitude of TEC. At 1200–1700 LT, the EIA was well-formed, particularly from 1400–1700 LT and the magnitude of the southern crest was higher than that of the northern crest, but conversely at 1200 and 1300 LT. At 1800–2300 LT, there was a reversal; the magnitude of the northern crest was higher than that of the southern crest, and plasma was localized around the magnetic equator with a single peak at 2300 LT. We also observed secondary minor peaks at ~±45o magnetic latitudes. The daily metamorphosis of the EIA structures followed the same morphologies during quiet- and storm-time, except for the storm effect on the EIA crests in terms of: expansion/increase in TEC or decay/decrease in TEC as may be dictated by whether the minimum main phase of a storm occurred at daytime or at nighttime.

Space Weather Applications & Services, Storm Effects, Equatorial Dynamics & Drivers, Equatorial Irregularities, High Latitude Structure & Irregularities

Sporadic-E and GNSS Scintillation

Beach, Theodore *Institute for Scientific Research, Boston College, Chestnut Hill MA, USA*

Multiple recent reports have claimed observations of daytime L1 band (1.6 GHz) amplitude scintillation associated with sporadic-E from ground-based GNSS measurements. While there is a long history of detecting ground-

Using the Ionosphere to Amplify Whistlers and EMIC Waves from Ground Transmitters for Reduction of Radiation Belt Particle Populations

Bernhardt, P.A., (2021) The Whistler Traveling Wave Parametric Amplifier (WTWPA) Driven by an Ion Ring-Beam Distribution from a Neutral Gas Injection in Space Plasmas, IEEE Transactions on Plasma Science. 49, 6, 1983-1996.

Hua, M., Bortnik, J., Ma, Q., & Bernhardt, P. A. (2022). Radiation belt electron acceleration driven by Very-Low-Frequency transmitter waves in near-Earth space. Geophysical Research Letters, 49, e2022GL099258.

Bernhardt, P. A., Hua, M., Bortnik, J., Ma, Q., Verronen, P. T., McCarthy, Ma6l Rd-10 (M)-11, Ma. Active precipitation of radiation belt electrons using rocket exhaust driven amplification j -5 (R)-1 (E)3 (

Space Weather Applications & Services, Active Experiments

receivers. Processed data may yield an image of the space debris traveling across the radio sky. The SOIMOW team is conducting experiments to determine if stimulated scatter from the UAF HAARP high power, ground-based transmitter can be employed to observe the trajectories of satellites and space debris.

P.A. Bernhardt, L. Scott, A. Howarth, G. J. Morales, Space Object Identification by Measurements of Orbit-Driven Waves (SOIMOW), Submitted to Physics of Plasmas, 2023.

Space Debris Monitoring and Remediation

HF scattering of ocean waves using HAARP

Briczinski, Stanley   *Naval Research Lab*

Coombs, Joseph NRL

Siefring, Carl NRL

The Variable Voltage Ion Protection Experiment (VVIPRE): Thermospheric and Ionospheric Remote Sensing from the ISS

Budzien, Scott Naval Research Laboratory

Dymond, Kenneth (NRL)

Fritz, Bruce (NRL)

Nicholas, Andrew (NRL)

Stephan, Andrew (NRL)

Wagner, Ellen (NRL)

VVIPRE is a demonstration space experiment built by the U.S. Naval Research Laboratory to show how low-cost variable voltage power supplies can protect sensitive spaceflight detectors from space plasma ion damage, extend sensor lifetimes, and deliver high-quality measurements of the Earth's upper atmosphere. Spacecraft charging and ambient ion impingement can cause noise, detector damage, and reduced sensor lifetime on-orbit. The variable voltage power supplies compensate for variations in spacecraft potential to reduce or eliminate this unwanted ion flow. Then naturally-occurring ultraviolet airglow can be measured to specify the atmosphere globally. VVIPRE will demonstrate successful ion mitigation by delivering space

Large Scale Traveling Ionospheric Disturbances in the Topside Ionosphere

Burrell, Angeline G   NRL

Dhadly, Manbharat Dhadly, (NRL)

Zawdie, Katherine (NRL)

Sassi, Fabrizio (NASA-GSFC)

Understanding the formation, progression, and global impact of Large Scale Traveling Atmospheric/Ionospheric Disturbances (LSTADs/LSTIDs) is a long-standing challenge in global space weather research. This has been a particularly perplexing problem due to the strongly coupled nature of the high-latitude ionosphere-thermosphere (IT) system, where they are believed to originate from. At high latitudes, the magnetosphere dumps a large amount of energy (both directly and indirectly) into the IT system through Joule heating, auroral particle heating, and ion drag. LSTADs are a commonly observed thermospheric response to magnetospheric energy entering the IT system. It is believed that LSTADs drive a similar wave response in the ionosphere, known as LSTIDs. Recent studies suggest that LSTADs/LSTIDs may also play an important role in transporting high-latitude variability to lower latitudes.

This study examines the impact of LSTIDs propagating from higher latitudes on the topside equatorial ionosphere. The altitude variation of LSTIDs is investigated using a combination of observational and modeling methods. The geomagnetic storms that occurred on the 23-25 March 2014 are used as a case study, as several Low Earth Orbit (LEO) satellites with orbits at different altitudes in the topside ionosphere were operational. The variations seen in the observations are then explored using model runs, which further allow a more detailed analysis of altitude variations once their variations are validated against the observational data.

HF Modeling, TIDs and Geolocation, Topside & Plasmasphere

A Limb-to-disk Algorithm for Mapping Scintillation Observations Along Radio Occultation Ray-paths to the Vertical Propagation Geometry

Carrano, Charles[1], Keith Groves[1], William McNeil[1], Endawoke Yizengaw[1], Paul Straus[2], Ron Caton[3], and Dallin Smith[3]

[1]Boston College Institute for Scientific Research, [2]Aerospace Corporation
[3]Air Force Research Laboratory

Modern radio occultation (RO) receivers such as the TGRS instrument onboard the COSMIC-2 satellites can routinely provide high-rate observations during ionospheric scintillation. TGRS, for example, provides 50 Hz and 100 Hz samples of amplitude and phase for GPS and GLONASS transmissions, respectively, whenever an elevated S4 triggers downlink of the occultation. The high-rate data enables direct measurement of the amplitude and phase scintillation indices (S4 and sigma-phi) as well as indirect (model-inferred) estimation of turbulence strength integrated along horizontal radio-occultation ray-paths. While useful, a ground-based user of satellite radio services (for communications, navigation, radar, etc.) would generally prefer to know the scintillation indices along a space-to-ground propagation path, possibly at a different operating frequency than TGRS uses to remote sense the ionosphere.

This paper presents a new limb-to-disk (L2D) algorithm for mapping scintillation along radio occultation ray-paths from the horizontal to the vertical propagation geometry. Since both turbulence strength and propagation distance contribute to the measured RO S4, it is necessary to first locate the irregularity region before the horizontal to vertical mapping is performed. The L2D algorithm accepts, as input, bubble geolocations from the Boston College TGRS Geolocation product, which which was developed and validated under the COSMIC-2

Radio Occultations & Tomography

An Improved Starting Field for Full Wave Modeling of High-Frequency Propagation in the Ionosphere

Carrano, Charles S.[1], Charles L. Rino[1], Louis Fishman[2]
[1]Boston College
[2]Tulane University

In a recent paper at the 2022 Beacon Satellite Symposium, we demonstrated that split-step Fourier methods, commonly implemented via the multiple phase screen technique, are unable to accommodate the large bending angles that occur when high-frequency (HF) waves propagate in the ionosphere. Alternative approaches that can accommodate these large bending angles include the split-step Padé method (Collins, JASM, 1989), a high-frequency operator symbol construction derived from phase space path integral methods (Fishman & McCoy, ASA, 1987), and a uniform high frequency operator symbol construction that is extremely accurate over a substantial parameter space (Fishman et al., WM, 1997). Each of these techniques require a starting field to initiate the computation. For a ground-based antenna that transmits a confined beam into the free-space region below the ionosphere, there is no difficulty initializing the computation if the beam radiates no appreciable energy at ionospheric altitudes as it enters the computational grid. However, in most HF applications the transmit pattern is broad and energy radiates essentially in all directions. In that event, a starting field that accommodates both the boundary conditions and the interaction with the ionosphere is required to initialize the computation. In the computational acoustics community, the PE self-starter proposed by Collins is widely used for this purpose (Collins, ASA, 1992; Collins, ASA, 1999). When applied to ionospheric problems, however, the PE self-starter does not properly model the scatter of energy by the extremely large propagation angles needed to reach the ionospheric region directly above the source. Orienting the reference direction toward the zenith could potentially mitigate this problem, but at the expense of increasing the range-dependence of media variations (which would increase the overall computational effort). For near vertical incidence skywave (NVIS) propagation problems, where one is interested in both vertical and downrange propagation using an exact representation of the Green's function for an Epstein (sech squared) ionospheric profile and perfectly conducting boundary conditions implemented via the method of images.

HF Modeling, TIDs and Geolocation

Modeling the Day-to-Day Variability of Midnight Equatorial Plasma Bubbles with SAMI3/WACCM-X

Chou, Min-Yang NASA GSFC, CCMC

Yue, Jia (NASA GSFC)

Validating and Improving a Realistic Ionospheric Truth Model for Observing System Simulation Experiments of HF Propagation

Collett, Ian   Orion Space Solutions

Hughes, Joseph (Orion Space Solutions)

Wilson, Walter ""Junk"" (Orion Space Solutions)

Crowley, Geoff (Orion Space Solutions)

Colman, Jonah (AFRL)

Landry, Russell (AFRL)

The US Air Force Cover Analysis Program (AFCAP) experiments 1, 2, and 3 have all been multimillion dollar campaigns to perform detailed Observing System Experiments (OSEs) of the ionosphere. Much of that expense has been dedicated to collecting enough observations of the ionosphere to be capable of post processing a “truth” ionosphere that supports additional analysis of alternative OSE experiments. Even after such great expense, significant limitations exist in the regional, seasonal, and decadal breath of available “truth” data. The ability to conduct a quality OSE without having to deploy dozens of sensors and dozens of people to the field would vastly expand the research opportunities across time and location. Such “virtual” OSEs are called Observing System Simulation Experiments (OSSEs) and require a synthetic truth model. For the HF propagation environment relevant to AFCAP, the synthetic truth model must accurately represent small-scale structures that are not present in smooth climatological or physics-based models. These small-scale structures must be physically realistic in both space and time to support OSSEs based on HF propagation. We present a synthetic truth model that attempts to meet these requirements and a path of further development which we believe will achieve this objective.

Our synthetic truth model is constructed from the smooth physics-based Thermosphere Ionosphere Electrodynamics General Circulation Model (TIE-GCM), by incorporating spatial and temporal electron density variations informed by two years of ionosonde measurements at mid-latitudes. The variations present in the ionosonde data that are not resolved by TIE-GCM are stored in terms of vertical, horizontal, and temporal correlations. To produce a realization of the truth model with these realistic electron density variations, to process is to (1) create uncorrelated Gaussian white noise, (2) use a Gaussian kernel in the spatial domain to enforce the vertical and horizontal correlations, (3) transform to the frequency domain to enforce the temporal correlation, and (4) apply this correlated noise to the TIE-GCM parent model.

Recently, using data from AFCAP experiment 2 (AE2), we have performed validation of the truth model’s re of the HF propagation environment. The AE2 data include oblique and vertical incidence soundings with a nominal 15-minute cadence. Ionospheric irregularities manifest as higher frequency variations in the time series of the maximum useable frequency (MUF) of oblique links. For several links of ground distances 500-2000 km, we perform OSSEs (HF raytracing through TIE-GCM and a realization of the truth model) to produce synthetic measurements for comparison. Although the time series observations are not the same because of the random nature of the truth model, we can compare spectral characteristics of the MUF. While the MUF spectrum for TIE-GCM falls off much quicker than the data, the spectrum for the realistic truth model matches the observed MUF spectra much more closely. Further methods of validation, such as a comparison of the E and F1 layer characteristics between the truth model and AE2 vertical incidence observations, are being pursued.

Improvements to the truth model are being explored. As previously described, the current version of the truth model is created by applying the spatial correlations with a Gaussian kernel and applying the temporal correlation in the frequency domain. We are pursuing an alternative approach using a coupled 4D spectrum of the ionosonde electron density variations that can be enforced in a single consistent step. We have developed numerical code for an N-dimensional Lomb-Scargle Periodogram that can reliably resolve spectral information from a set of non-uniform measurements in both space and time, enabling this kind of approach. In principle, the

Over-the-horizon (OTH) Propagation: Ray Trace Model and Measurement Matching

Conroy, James JHU APL

Ellison, Sean (JHU APL)

McFadden, Francesca (JHU APL)

Wiker, Jordan (JHU APL)

Outwater, John (JHU APL)

Predicting the propagation of high frequency (HF) radio wave power from a transmit to a receive

Solar Cycle 25: Analysis of Recent Space Weather Events

Coster, Anthea J *MIT Haystack Observatory*

Aponte, Nestor, (MIT Haystack Observatory)

Zhang, Shun-Rong (MIT Haystack Observatory)

Goncharenko, Larisa, (MIT Haystack Observatory)

Derghazarian, Sevag, (MIT Haystack Observatory)

Solar cycle 25 began in December 2019 and was predicted to have a sunspot range between 95 to 130 with the solar maximum occurring between 2023 and 2026. Although these predictions led people to forecast similar activity levels to solar cycle 24, observations from 2020 to 2023 have significantly exceeded the anticipated values. For example, during the first month of 2023, sunspot numbers were around 185, much higher than the peak values of 95 to 130 predicted. Also in January 2023, the daily F10.7 values exceeded 220 and there were 3 X class solar flares. One day in February 2023, the daily F10.7 exceeded 300. With this in mind, we will report on observed space weather activity in 2022 and 2023 related to these heightened activity levels. We will utilize data in the Madrigal database including the total electron content (TEC) observations from the global ground-based network of GNSS receivers and scintillation statistics obtained from networks of specialized GNSS receivers. These networks include: the NSF MRI Collaborative: Development of Monitors for Alaskan and Canadian Auroral Weather in Space (MACAWS), the Canadian High Arctic Scintillation Network (CHAIN), the Low-Latitude Ionospheric Sensor Network (LISN), and in the Istituto Nazionale di Geofisica e Vulcanologia (INGV) network. New software will be used to merge the GNSS TEC maps and scintillation observations. In addition, optical observations from the THEMIS all-sky imaging network which measure the auroral activity and SuperDARN convection maps will be incorporated into our analysis of recent space weather events. Recent solar flares, large 2022 and 2023 geomagnetic storms and substorms, and specific scintillation events associated with storm enhanced density plumes, tongues of ionization, and auroral substorms will all be analyzed. Observed differences in space weather activity between the hemispheres will be highlighted. We will also examine the role of the higher levels of solar activity (F10.7) in the development of space weather phenomena.

Storm Effects, High Latitude Structure & Irregularities

Interpreting the Doppler shift of Transionospheric HF radio waves

Danskin, Donald University of Saskatchewan

Gillies, Rob (University of Calgary)

Eyiguler, E. Ceren (University of Saskatchewan)

Pandey, Kuldeep (University of Saskatchewan)

Hussey, Glenn (University of Saskatchewan)

Yau, Andrew (University of Calgary)

The radio receiver instrument (RRI) on the e-POP/Swarm-E satellite is affected by the motion of the satellite causing a Doppler shift in the received frequency. Traditionally, to determine the Doppler shift, only the motion of the receiver relative to the transmitter is necessary. However, when traveling through a dispersive medium such as the ionosphere, especially for radio waves in the HF band, the changing refractive index needs to be considered. Using a raytracing method, the refractive index is determined for an electron density profile along the path of the radio wavoor(<</MCIo r9 -1.2)2 (enc)-10 (r6 (nuCIo r)-1 (Td [(r n)-4 (s)-5 (t)a)-1 (i)-6 (l(r)-1)-1 (at-1 (a

The Onset and Development of Nitric Oxide Production During ICME-Driven Storms

Delano, Kevin University of Maryland, Baltimore County (UMBC)

Oliveira, Denny (UMBC/Goddard Space Flight Center)

Zesta, Eftyhia (Goddard Space Flight Center)

Enhanced thermospheric nitric oxide (NO) production regulates the interplay of neutral mass density heating and cooling, which in turn affects neutral density predictions, a crucial component of satellite orbital drag forecasting. However, the onset of NO production and its subsequent spaciotemporal development during storm times remains poorly understood. Using the Sounding of the Atmosphere using Broadband Emission Radiometry (SABER) instrument on the Thermosphere, Ionosphere, Mesosphere Energetic Dynamics (TIMED) spacecraft, we investigate NO production during 13 moderate geomagnetic storms (minimum SYM-H between -50 and -

Connections Between Stratospheric and Mesospheric Gravity Waves, Winds and Traveling Ionospheric Disturbances

Derghazarian, Sevag MIT Haystack Observatory

Goncharenko, Larisa P. (MIT Haystack Observatory)

Zhang, ShunRong (MIT Haystack Observatory)

Coster, Anthea J. (MIT Haystack Observatory)

Harvey, V. Lynn (University of Colorado Boulder, LASP)

Randall, Cora (University of Colorado Boulder, LASP)

We present evidence that stratospheric gravity waves (GWs) are imprinted on the thermosphere

The importance of electric field in ions convergence and formation of sporadic E (Es) at the equatorial region

Didebulidze, Goderdzi

Ionospheric response to the 23–31 August 2018 geomagnetic storm in the Europe-African longitude sector using multi-instrument observations

Dugassa, Teshome *Space Science and Geospatial Institute, Ethiopia*

Nigussie Mezgebe (Space Science and Geospatial Institute Ethiopia)

John Bosco Habarulema (South African National Space Agency)

This study presents ionospheric responses of the mid and low-latitude region in the Europe-African longitude sector (along 30oE±10oE) to the intense geomagnetic storm of 23–31 August 2018 (SYM-Hmin = -207 nT) using the Global Ionospheric Map (GIM) and Global Positioning System (GPS) receivers data, the satellite data (SWARM, Defense Meteorological Satellite Program (DMSP), Global Ultraviolet Imager on board the Thermosphere, Ionosphere, Mesosphere Energetics and Dynamics (GUVI/TIMED)), and Prompt Penetration Equatorial Electric Field model (PPEFM). The percentage deviation in total electron content (TEC) denoted by DTEC (%) was used to observe the ionospheric storm effects. The rate of change of TEC index (ROTI) derived from GPS-TEC and the rate of change of plasma density index (RODI) obtained from SWARM satellites were utilized to quantify the occurrence of ionospheric irregularities. Results obtained from GPS receivers and GIM data revealed a large increase in TEC (positive ionospheric storm effect) in the equatorial and low-latitude region of Africa, and a decrease in TEC (negative ionospheric storm effect) over the midlatitude region of Europe and Africa during the storm recovery phase. The decrease in ½O=½N 2 ratio is the possible cause for the observed negative ionospheric storm effect. Hemispheric asymmetry were noticed over EuropeAfrican longitude sector during the storm main and recovery phases. The occurrence of ionospheric irregularities over the low-latitude region of Africa in the premidnight and post-midnight was(c)-6 (4 (r)2 ((n)2 (a)42. (ovec66 (e)-13 ((R (T)½O4 (9)-121 T)<ovec0.42 (n T)1 (E)1 (C

Combining Ground- and LEO-RO-Based GNSS Observations in Real-time Operational Space Weather Products

Durgonics, Tibor[1,2], Tzu-Wei Fang[1], Terry Onsager[1], Frank Centinello[1], Jun Wang[2], Dominic Fuller-Rowell[1,2], Mihail Codrescu[1]

[1] NOAA Space Weather Prediction Center

[2] Cooperative Institute for Research in Environmental Sciences, CU Boulder

NOAA's Space Weather Prediction Center (SWPC) has responsibility for continuously monitoring, forecasting, and alerting on conditions in the Earth's space environment that impact our technological infrastructure and human health and safety. One of the main space weather products is the ionosphere specification. Ionospheric density changes impact our technologies utilizing global navigation satellite systems (GNSS) and signals propagating between satellites and the ground stations as it can cause signal delays and disruptions. SWPC focuses on improving existing and creating new real-time, operational products of the two main ionospheric descriptive quantities: total electron content (TEC) and ionospheric scintillations. SWPC is also one of the centers that are responsible for space weather services identified by the International navigation, thus providing society with actionable space weather information. The main challenges are currently being addressed in close collaboration with Boston College and Aerospace Corp.: 1) the validation of ground-based scintillation measurements, 2) geolocation of RO scintil

Topside Ionosphere Electron Density Modeling with Empirical and Machine Learning Techniques

Dutta, Shweta Georgia Institute of Technology

Cohen, Morris (Georgia Institute of Technology)

This research focuses on modeling the electron density in the topside of the ionosphere with a combination of a developed machine learning model and existing empirical models, specifically the International Reference Ionosphere (IRI) and the Empirical-Canadian High Arctic Ionospheric Model (E-CHAIM). In prior work, an artificial neural network (NN) was developed and trained on two solar cycles worth of Defense Meteorological Satellite Program (DMSP) data (113 satellite-years), along with global drivers and indices to predict topside electron density. We tested the model on six years of subsequent data (26 satellite-years) and found a correlation coefficient of 0.87 between the model predictions and the DMSP electron density data. While the NN model outperforms the IRI when tested on data in the altitude range the NN was trained on, performance is degraded in the polar region and during elevated solar activity when testing on a dataset sourced from a lower altitude satellite. Now, we present analysis of the matured NN model, E-CHAIM, and IRI by geographic location and geomagnetic condition within the topside ionosphere, and preliminary work to combine all three models via stacked generalization.

Topside & Plasmasphere

The Experiment for Characterizing the Lower Ionosphere and Prediction Sporadic-E (ECLIPSE) Missions: Instruments to Study the Dynamics of the Lower Ionosphere

Dymond, Kenneth F. U.S. Naval Research Laboratory

Andrew C. Nicholas, Bruce A. Fritz, Scott A. Budzien, Andrew W. Stephan, Charles M. Brown, Ellen J. Wagner, Meghan R. Burleigh, and Douglas P. Drob

U.S. Naval Research Laboratory, 4555 Overlook Ave, Washington, DC, 20375, USA.

The Naval Research Laboratory designed and developed small instruments for flight on CubeSats to study the Earth's ionosphere. One instrument is a photometer, called the Tiny-Triple Ionospheric Photometer (Tri-TIP), used to measure the brightness of the O I 135.6 nm emission produced primarily by radiative recombination of O+ ions and electrons. At nighttime this emission can be used to infer the distribution of electrons in the ionosphere. A second instrument, called the Triple-Magnesium Ion Photometer (Tri-MIP), is designed to measure the Mg II 280 nm emission, which is produced during the daytime by scattering of sunlight by Mg+ ions in the ionosphere. Mg+ ions are produced by meteoric ablation and also by charge exchange between molecular ions and Mg atoms produced during the meteor ablation. Mg+ ions act as tracers of the dynamical drivers in the E- and F-regions of the ionosphere. Prior measurements of both species have been used to determine the two-dimensional distribution of the ions in the orbit plane of the satellite making the measurements.

In this talk, we will describe the observations of the Tri-TIP and Tri-MIP instruments on two missions. A prototype of the Tri-MIP instrument was built and launched on a new CubeSat mission (ECLIPSE-RR) into low Earth orbit to study the spatial distribution of Mg+ ions. The satellite (SLINGSHOT-1), a collaboration with the Aerospace Corporation, was launched out of Southern California on the Virgin Orbit launch that occurred on July 2, 2022. The orbit is circular at an altitude of 555 km and an inclination angle of 45°. The second mission, ECLIPSE, will fly two Tri- MIPs and two Tri-TIPs on the United Space Force Space Test Progra (a (a (-ma)6 (k)2s)

Comparisons of the Data-Driven D Region (D3R) Model to Incoherent Scatter Radar Observations During the Active Solar Conditions of September 2017

Egert, Austin   Space Dynamics Laboratory

Eccles, James V., Space Dynamics Laboratory;

Holmes, Jeffrey M., Air Force Research Laboratory;

Malins, Joseph, Air Force Research Laboratory

The physics-based Data-Driven D-Region (D3R) model calculates electron density profiles from 40 to 130 km for quiet time and disturbed conditions. The D3R model has recently been updated with the following: (1) additional positive and negative ions, similar to the 8-component scheme of Bekker et al. (2022), (2) updated reaction rates presented in Pavlov (2014, 2015), (3) the Flare Irradiance Spectral Model

HF Propagation & Systems

Operational Assimilative Ionospheric Models in Europe and the UK

Elvidge, Sean SERENE, University of Birmingham

Themens, David (SERENE, University of Birmingham)

Comprehensive, global and timely specifications of the Earth's ionosphere is required to ensure the effective operation, planning and management of a diverse range of systems impacted by space weather. This year, a number of national space weather operational centres are deploying ionospheric data assimilation models operationally.

The UK Met Office Space Weather Operations Centre (MOSWOC) runs the Advanced Ensemble electron density (Ne) Assimilation System (AENeAS), a physics-based data assimilation model of the coupled ionosphere-thermosphere system. AENeAS assimilates data using the local ensemble transform Kalman filter (LETKF) into a background model (the Thermosphere Ionosphere Electrodynamics General Circulation Model [TIE-GCM]). The model provides probabilistic environmental nowcasts and forecasts, as well as tailored products and services to support industry and Government.

The European Space Agency's Space Weather Service Network will run the Advanced Ionospheric Data Assimilation (AIDA) model pre-operationally. AIDA uses a modified Auxiliary Particle Filter to assimilate data into the climatological NeQuick model. Unlike most global data assimilation models, AIDA uses basis functions as its state space to drastically reduce its size and describes the forward model via analytical functions rather than discrete voxels. These computational savings allow for the use of a more intensive assimilation method, for example APFs, which are more flexible and can incorporate highly non-linear datasets.

Space Weather Applications & Services, Assimilative and Coupled Models

Assimilative Modeling of the Ionospheric Layers

Forsythe Victoriya *NRL*

McDonald, Sarah (NRL), Kuhl, David (NRL), Fritz, Bruce (NRL), Diamond, Ken (NRL)

A new data assimilation (DA) scheme for the parametrized ionospheric electron density is currently under development at the Naval Research Laboratory (NRL). It provides the nowcast for the given ionospheric background model influenced by ionospheric observations, using sequential Kalman Filter on the maps of the ionospheric parameters in Quasi-Dipole MLT coordinate system. During this presentation, this new DA scheme, the covariance formation and the data aggregation will be introduced. The pre-processing technique for three data types, ionosonde, radio occultation, and ground-based GPS data, will be described. First results and preliminary validation efforts, including the comparison with IDA4D results will be demonstrated.

This work is sponsored by the Office of Naval Research.

Assimilative and Coupled Models

First-year Results from a Space-based Sporadic-E Detector

Fritz, Bruce U.S. Naval Research Laboratory

Dymond, Kenneth (U.S. Naval Research Laboratory),

Nicholas, Andrew (U.S. Naval Research Laboratory),

Budzien, Scott (U.S. Naval Research Laboratory),

Stephan, Andrew (U.S. Naval Research Laboratory)

The Triple Magnesium Ionospheric Photometer (Tri-MIP) has been developed as a 1U CubeSat compatible sensor to detect a mid-ultraviolet (MUV), Mg+ doublet emission near 280 nm as a tracer of Es. The initial flight of Tri-MIP is on the Slingshot-1 spacecraft that launched into a circular orbit at an altitude of 500 km and an inclination of 45º. Paired with a 1U scanning ultraviolet mirror (SUVM) on the Slingshot-1 spacecraft, Tri-MIP provides altitude profiles of Mg+ airglow emissions through limb scans of Earth's ionosphere along the wake direction of the orbit. Tri-MIP is especially well-suited for Es detection and may allow for the observation of faint signatures of Es that are otherwise not visible with other commonly used, plasma detection methods, such as ground-based ionosondes or GPS radio occultation experiments. This will show the data reduction approach that is being applied to the observations as well as a summary of results from the first year of operations on orbit.

The Incorporation of Near Real Time Ionospheric Propagation Information for Automated Link Establishment Based Communication Systems

Furman, William *L3Harris Technologies, Inc.*

Batts, William (L3Harris Technologies, Inc.)

Buckley, Richard (L3Harris Technologies, Inc.)

Nieto, John (L3Harris Technologies, Inc.)

This paper focuses on the use of the HF frequency band, 3-30 MHz, as a wireless communications medium where the predominant propagation mode is provided by ionospheric refraction. The HF medium provides a reliable mode of long distance, beyond line of sight, communications used by many nations and entities worldwide.

The paper begins with an overview of existing Automated Link Establishment (ALE) systems which provide a mechanism to find the best propagating frequency between any radios on earth and to set up the radios for communication. The paper will provide a brief history of ALE throughout the years up to and including the current U.S. MIL-STD-188-141D.

Next the use of propagation prediction software is discussed with a concentration on VOACAP. This package provides a prediction of the best propagating frequency between points on earth based many factors including geographic positions, time of day, solar activity, and noise conditions. VOACAP is generally used to select possible / probable frequencies to use before radios are deployed in the field but does not have a mechanism to address real time variations in propagation.

Sources of Near Real Time (NRT) propagation information are then discussed . This information includes WWV broadcasted geomagnetic and solar indices information, inputs from space weather organizations, and amateur radio propagation probing waveforms such as WSPR.

A comparison of various waveforms for real time channel evaluation is then presented. Examining waveforms used by the US M(nc)43nf us T7.49sinadio pr usvameec (pl)-2 (o)520 (y) usnga

A Vertically-Resolved Model for Ionospheric Absorption of HF radio waves due to solar protons and X-rays

Goertz, Anton Los Alamos National Laboratory

Jeffery, Christopher (Los Alamos National Laboratory)

High Frequency (HF) skywave radio signals are used in various communication technologies and commonly pass through the D-Region ionosphere. Enhanced levels of D-Region ionization during geomagnetic storms can cause partial or even complete absorption of HF radio waves leading to communication disruptions and blackouts. This ionization is predominantly caused by solar energetic protons (SEP) and solar X-rays precipitating into the ionosphere. To better predict this process, we have developed a new vertically-resolved model to determine the absorption of HF waves due to SEPs and solar X-rays. Our model explicitly resolves the altitude-dependence of high rays. Our model exp (a((a(J 0 Tc 0 Tc 0-Tw 120 Td [(r)-0.33 0 e0 Tc 0 5 2 (g)1d3 (r)3 tu)2 (d)2 (e)]TJ 0

An Empirical Mid -Latitude Model of the CkL Irregularity Index from 35 MHz Scintillation Data

Helmboldt, Joseph U.S. Naval Research Laboratory

the DLITE-based model at the irregularity locations. This trend is not present when WBMOD CkL values are used. While the two measurements probe different portions of the irregularity spectrum, this result still indicates that utilizing up-to-date regional scintillation data can improve irregularity nowcasting and forecasting at mid-latitudes.

Scintillation & Propagation Effects on GNSS and Other Systems

Simultaneous Measurements of Temporal and Spatial Phase Structure Functions of an HF Skywave Signal at Mid-Latitudes

Helmboldt, Joseph *U.S. Naval Research Laboratory*

Data-Assimilative Ionospheric Profile Specification Using Scaled IRI Parameters

Hoskinson, A. R., V. Paznukhov, W. J. McNeil, M. Proctor, C. S. Carrano, and K. M. Groves

Institute for Scientific Research, Boston College

We present a regional data-assimilative ionospheric model, the Region Ionospheric Profile Estimator (RIPE) that aims to improve the specification of bottom-side electron density profiles by updating individual profile parameters of the International Reference Ionosphere (IRI) based on measured ionosonde data. Our approach operates on the *ratios* of auto-scaled parameters to climatological model predictions for f_oF2 (URSI model), $hmF2$ (Shubin), and B_0 and B_1 (Altadill, Torta, and Blanch). This approach allows the dominant spatial and temporal structure in the ionosphere to be handled by well-validated climatological models, while the data
-strbes (.6 (A4 Td p(r)3 (of)3 (i)-2 (l)-2 (e)4 (ph)-10 (a)4 or)3 (a)-6 (m)-2 (e)4 (t)-2 (e)4 (r)3 (s)-1 (t)-2 (

Modeling Plasmasphere Structure: Ducts and Irregularities

Huba, Joe *Syntek Technologies*

Liu, H.-L., HAO

Becker, E., NWRA

We present results from high-resolution simulations of the thermosphere-ionosphere-plasmasphere system using the coupled SAMI3/WACCM-X and SAMI3/HIAMCM models. We show that atmospheric gravity waves can generate plasma irregularities and ducts in the plasmasphere. High resolution simulations using SAMI3 with the empirical models NRLMSISE00 and HWM14 of the thermosphere do not show any density structuring. We demonstrate that field-aligned ducts (i.e., localized density enhancements or reductions) can form in the mid-latitude ionosphere by calculating the flux-tube integrated total electron content (in contrast to vertical total electron content). We find that there can be variations of a few percent over a few degrees in longitude. We also discuss how these results may apply to plasmasphere irregularities observed by radio astronomy facilities as well as to VLF propagation studies.

Topside & Plasmasphere

A Verification and Validation of the Observation System Simulation Experiment Tool

Hughes, Joe   Orion Space Solutions

Collett, Ian (Orion Space Solutions)

Reynolds, Adam (Orion Space Solutions)

Crowley, Geoff (Orion Space Solutions)

Decision makers are often tasked with choosing how many sensors to deploy, of what types, and in what locations to meet a given operational or scientific outcome. An Observing System Simulation Experiment (OSSE) is a numerical experiment which can provide critical decision support to these complex and expensive choices. There are three steps in an OSSE:

(1) An observation system consisting of any combination of instruments such as ionosondes, GPS ground stations, satelli-

MF Scattering from the Exponential D-Region: Analytic Theory & Double-Peaked Ground Signatures

Jeffery, Christopher   Los Alamos National Laboratory

MF Scattering from the exponential D-Region is investigated analytically using the geometrical optics approximation. Expressions for scattered-ray path and amplitude are derived and used to interpret results of frequency-domain full-wave simulations with km-scale regions of imposed stochastic variability. The simulations reveal double-peaked ground signatures that appear consistent with the dual Doppler structures seen by Obenburger et al. (Radio Science, 2022). Analysis reveals that the far peak is due to refraction, while the near (transmitter-ward) peak is caused by scattering of rays that first ionospherically reflect. The contribution of horizontal, near-caustic scattering to the latter peak from plasma variability at the reflection height is further clarified.

HF Modeling, TIDs and Geolocation

Development of an Autonomous RF System that exploits SuperDARN Signals for Bistatic Radar Imaging of High-Resolution Ionospheric Structures near HAARP

Jeffery, Christopher   Los Alamos National Laboratory

Shao, Xuan-Min (LANL)

Beveridge, Andrew (LANL)

Cummings, Ian (LANL)

Cunningham, Greg (LANL)

Fallen, Christopher (AFRL)

Haynes, Brian (LANL)

Lay, Erin (LANL)

Nelson, Eric (LANL)

Reisner, Jon (LANL)

Rushton, Jeremiah (LANL)

LosTj EMC5.75 0 Td ( )T0.01 d [Tw [(R)22 -12.46iLN ((al)-2tioyopLn (L eale Td i4 8 (Ldl)-2 ()-2vlee)LL t

High frequency surface wave oceanographic research radars as bistatic single frequency oblique ionospheric sounders and day-to-day ionospheric variability

Kaeppler, Stephen *Clemson University*

Miller, Ethan (STR)

Markowski, Danielle (Clemson University)

Coleman, Lawrence (Clemson University)

We demonstrate that bistatic reception of high frequency oceanographic radars can be used as single frequency oblique ionospheric sounders. We develop methods that are agnostic of the software defined radio system to estimate the group range from the bistatic observations. The group range observations are used to estimate the qtiat op mq- (a)4frrgstno4 (f)3 (r)nrsic oa (op m)-2
s

Generation of Realizations of Electron

Using GNSS instantaneous phase differential to geolocate acoustic sources from August 2022 bolide

Lay, Erin *Los Alamos National Laboratory*

Tippmann, Jeff

Shao, Xuan-Min

Haaser, Robert

The ubiquity of GNSS receivers world-wide has led to many advances in ionospheric monitoring fairly inexpensively, and on a global scale. In this talk, we demonstrate the application of an instantaneous phase differential technique to geolocation acoustic wave sources in the ionosphere using high-rate (1-second cadence) ground-based GNSS measurements. We have applied the technique to the bolide that exploded over Northern Utah on 13 August 2022. The technique locates a path of the acoustic wave perturbations that is consistent with observations on the ground. We also discuss the limitations we discovered in application of the technique to this bolide case.

HF Modeling, TIDs and Geolocation

Ionospheric Effects of Geospace Storm 5-6 August 2019

Luo, Yiyang V. N. Karazin Kharkiv National University

Chernogor, Leonid (V. N. Karazin Kharkiv National University)

Garmash, Konstantin (V. N. Karazin Kharkiv National University)

Guo, Qiang (Harbin Engineering University)

Zheng, Yu (Qingdao University)

The urgency of this work lies in the complex and synergistic nature of geospace storms, which involve interactions between magnetic, ionospheric, and atmospheric storms in the magnetospheric, ionospheric, and atmospheric environments. Since no two geospace storms behave exactly alike, it is crucial to study the effects of each new storm in order to reveal both the general laws and individual characteristics of storm processes. The purpose of this paper is to present general information about geospace storms and to analyze the features of magnetic and ionospheric storms. To analyze the magnetic environment, we used measurement results of magnetic field fluctuations in the range of 1 s to 1000 s from the Magnetometric Observatory of V. N. Karazin Kharkiv National University, as well as variations of the three components of the geomagnetic field from the Low-frequency observatory of the IRA NASU. To analyze the ionospheric environment, we used multi-frequency multi-path measurements performed at Harbin Engineering University (China), as well as ionosonde data. The main results of this work are as follows. An increase in the main parameters of the solar wind on August 5, 2019, led to a geospace storm that was mainly observed on August 5 and 6, 2019. The main phase of the magnetic storm occurred from UT 06:00 a.m. to UT 08:30 a.m. on August 5, 2019, while the recovery phase lasted at least 4 days. The magnetic storm exhibited significant variations in all components of the geomagnetic field, with an order of magnitude increase in oscillation levels of the geomagnetic field in the range of 400 s to 950 s. During the ionospheric storm, significant disturbances occurred in the F region of the ionosphere, while the E region of the ionosphere remained weakly perturbed. The ionospheric storm also severely affected the Doppler spectra of radio waves in the 5–10 MHz frequency range, with significant broadening of the spectra and quasi-

Ionospheric Effects During Moderate Earthquake in Japan on September 5, 2018

Luo, Yiyang V. N. Karazin Kharkiv National University

Chernogor, Leonid (V. N. Karazin Kharkiv National University)

Garmash, Konstantin (V. N. Karazin Kharkiv National University)

Guo, Qiang (Harbin Engineering University)

Shulga, Sergey (V. N. Karazin Kharkiv National University)

Zheng, Yu (Qingdao University)

The Earth's interior layers, atmosphere, ionosphere, and magnetosphere (EAIM) constitute an interconnected system that is open, dynamic, and nonlinear. The direct and reverse, positive and negative linkages among the subsystems within the EAIM system remain inadequately explored. A high-power release of energy from one of the subsystems can trigger interactions among the subsystems.

new features. In conclusion, we provide an overview of our JPL ionospheric products, their parameters, as well as the current and futures uses.

Coster & Komjathy, 2008, Space Weather and the Global Positioning System, Space Weather 6, https://doi.org/10.1029/2008SW000400.

Mannucci et al., 1998. A global mapping technique for GPS-derived ionospheric total electron content measurements, Radio Science 33 565-582, https://doi.org/10.1029/97RS02707.

Space Weather Applications & Services

Revisiting refractive contribution to radio wave scintillation for polar cap

Responses of the Nigerian low-latitude ionosphere to geomagnetic storms of the ascending and maximum phases of solar cycle 24

Oyeyemi, E.O.[1], A.O. Akala[1], D. Okoh, O.O. Odeyemi[1], B. Olugbon[1], P.O. Amaechi[1], O. J. Oyedokun[1], O.R. Idolor[1]

[1]Department of Physics, University of Lagos, Akoka, Yaba, Lagos, Nigeria

This study investigates the responses of the Nigerian ionosphere to thirteen geomagnetic storms that occurred during the ascending and maximum phases of the solar cycle 24. The Total Electron Content (TEC) data obtained from the Nigerian Global Navigation Satellite System (GNSS) network (NIGNET) were used for this study. The ionosphere over Nigeria recorded marked TEC variations around 1100–1700 LT with the highest values between 1400 LT and 1600 LT, and a minimum diurnal variation at 0600 LT. Another cogent piece of information from this study is that the values of TEC at all the five GNSS stations under investigation consistently matched one another. The implication of this is that the values of TEC, at both quiet time and storm time, at any location in Nigeria could be used as the representative values at any other locations in the country, particularly in areas where there are no GNSS systems. The equinoctial maxima and June solstice minima effects were clearly observed in our data. Furthermore, ionospheric irregularities occurrence also followed semiannual patterns with two peaks in April and October, and the least occurrences in June and Ooksr t-4 (cei)-2 (nl)2 (a) Tw [(aw)4

Changes in Polarization State of Transionospheric Radio Waves Driven by Difference in O- and X-mode Powers

Pandey, Kuldeep *University of Saskatchewan*

Kalafatoglu Eyiguler, E. Ceren (University of Saskatchewan)

Danskin, Donald W. (University of Saskatchewan)

Gillies, Robert G. (University of Calgary)

Yau, Andrew W. (University of Calgary)

Hussey, Glenn C. (University of Saskatchewan)

The Radio Receiver Instrument (RRI) of the Swarm-E/e-POP (eceii001 Tc)-3.3 (d)1(y)20 (i)20 (i(y)16 (o)1

A study of the relative dynamics of ionospheric irregularities and GPS satellites on receiver tracking performance from a low-latitude station in the Indian longitudes

Paul, Ashik *Institute of Radio Physics and Electronics, University of Calcutta*

Biswas, Trisani (Institute of Radio Physics and Electronics, University of Calcutta)

Dynamics of the low-latitude ionospheric irregularities can make transionsopheric satellite communication and navigation links vulnerable to medium introduced signal perturbation, sometimes to the extent of complete signal outage. Characteristics of the motion of satellites can introduce an additional metric in signal perturbation in relation to the drifting irregularity structures. This paper reports the relative contribution of GPS satellite geometry vis-à-vis irregularity movement on tracking loop performance of ground-based receivers during periods of ionospheric scintillations, observed from station Calcutta (22.58°N, 88.38°E geographic; magnetic dip 34.54°), located near the northern crest of Equatorial Ionization Anomaly (EIA). For this stud[(la)6 (ti)- (i)el pe (()3 (22. (g)10 (ul)2 (m)-6 (s)-d)4 (a)--2 (n)-10 (g)10 (pe)4 (r)3-2 (s)-(c)-

Automatic real-time tool for processing of oblique sounding data

Paznukhov, D., K. Kraemer, T. Beach, B. Drummond, M. Proctor, K. Groves

Boston College, Institute for Scientific Research, 140 Commonwealth Ave., Chestnut Hill, MA 02467

Dao, Eugene (AFRL)

We present a robust, flexible system for real-time automated oblique ionogram data trace extraction and electron density profile (EDP) parameter estimation manner with quality control and data filtering capabilities. The developed system, named Optimal Approach System for Ionogram Scaling (OASIS) performs an automatic extraction of oblique traces; infers the ionospheric profile parameters and assesses data quality, parameter uncertainty and confidence. A novel approach used in this work was application of modern optimization algorithms to implement automatic ionogram processing. The ionospheric parameters are extracted by minimizing the difference between the real ionogram measurements and the ones modeled with specific ionospheric characteristics. The uncertainties of the extracted parameters are estimated

Detrending GOLD EUV Data to Reveal Equatorial Plasma Bubble Structures

Pradipta, Rezy *Boston College, Institute for Scientific Research*

Groves, Keith (Boston College)

Huang, Chaosong (AFRL)

We report our investigation on the detection and classification of equatorial plasma bubble (EPB) structures in the Global-scale Observations of the Limb and Disk (GOLD) EUV data. We have developed a novel technique for detrending the nighttime GOLD EUV irradiance data, which helps reveal large-scale field-aligned depletions associated with EPBs. The data detrending technique is a two-dimensional generalization of the rolling-barrel data detrending technique [Pradipta et al., 2015] that operates in one dimension. In this case, the rolling barrel is replaced with a rolling ball with two degrees of freedom to navigate across a two-dimensional uneven terrain defined by the nighttime GOLD EUV irradiance data. The inferred baseline irradiance and the detrended irradiance data are subsequently transformed into geomagnetic coordinate in order to trace the position of the equatorial ionization anomaly (EIA) crests and the shape of EPB depletions. In the data analysis, the detected EPB depletions may appear either straight or curved with an inverse-C shape, depending on the solar local time. Zonal drift velocities of the detected EPBs are deduced based on sequential frames of GOLD EUV observation data. Afterwards, the computed EIA and EPB traces are transformed back from geomagnetic into geographic coordinate for realistic comparison with the original GOLD EUV observation data.

Sferic-based tomography for D-region imaging

Richardson, David *Georgia Institute of Technology*

*Cohen, Morris (Georgia Institute of Technology, mcohen@gatech.edu)

The lower ionosphere, in particular the D region (60-90 km), is difficult to reach with direct measurements (balloons, satellites, etc.) due to its altitude range. Instead, researchers have relied on very low frequency (VLF, 3-30 kHz) and low frequency (LF, 30-300 kHz) remote sensing techniques. Using these techniques, D-region ionosphere models have historically estimated electron density along transmitter-to-receiver paths, in particular path-averaged electron density While these techniques do provide useful geophysical information, they are somewhat lacking in terms of spatial information. Our work utilizes recent improvements in lightning-based path-average estimates in combination with tomography to produce 3D maps of electron density within the D-region ionosphere. During quiet time, we are able to produce daytime, nighttime, and day-night terminator electron density maps within our area of confidence (Gulf of Mexico and SE United States). Based on our results in a synthetic case, we estimate our error to be less than 10% within this region. During the 2017 solar eclipse, we also show strong agreement between our modeled electron density and the eclipse location demonstrating our model's ability to capture interesting geophysical phenomena. As this technique is developed further, it is our hope to include information from VLF transmitters into the model to unify exi-5 (s)-2 (i)t

Forward Propagation Geometrical Optics and Beam Steering

Rino, *Charles* *(1), Charles Carrano (1), and Keith Groves(1)
(1) Institute for Scientific Research, Boston College, Chesnut Hill, MA, USA

1 Introduction

The propagation of electromagnetic (EM) waves is governed by Maxwell's equations. Constitutive relations characterize the interaction of the electric and magnetic field with the medium. For the earth's ionosphere and atmosphere the constitutive relation is a frequency-dependent tensor or scalar. Vector wave equation follows from the time-harmonic form of Maxwell's equations upon neglecting the gradient of the electric-field divergence. For the purposes of this paper we consider the scalar form of the wave equation, which we write here in two forms:

$$\nabla^2\psi(x;\eta) + k^2\psi(x;\eta) = k^2X(x;\eta)\psi(x;\eta) \quad (1)$$

$$\left[\frac{\partial^2}{\partial x^2} + \nabla_{\perp}^2 + k^2K(x;\eta)\right]\psi(x;\eta) = 0 \quad (2)$$

where $K(x;\eta) = \sqrt{(n\,r)} = 1 + X(x;\eta)$ In the first form of the wave equation the term involving $X(x;\eta)$ acts as an induced source. The second form incorporates $X(x;\eta)$ within an operator that acts on the total field. The weak-scatter theory and the theory of propagation in stochastic media proceed from the first form of the wave equation. The multiple phase screen (MPS) method is often thought of as a guiding principle embodied in the forward propagation equation (FPE):

$$\frac{\partial\psi(x;\eta)}{\partial x} = \Theta(x;\eta) \quad K(x;\eta)/2\psi(x;\eta); \quad (3)$$

where $\Theta(x;\eta)$ is the free-space propagation operator.

In two recently published papers, [1] and [2], we extended the FPE to accommodate vector HF propagation, with encouraging results. However, as noted in the second paper, a disparity between vector forward propagation realizations and geometrical optics predictions was found. The disparity is the result of a fundamental constraint which limits [illegible] MPS methods to narrow-angle propagation. The limitation is well know in acoustic propagation where wide-angle extension of the narrow-angle scatter theory are used routinely. The HF applications will be discussed in a separate presentation. The remainder of this paper will discuss extensions of geometrical optics as a diagnostic intermediary.

For scalar fields geometric optics ray theory takes a particularly simple form:

$$\frac{d^2 r}{ds^2} + \frac{dn}{ds}\frac{dr}{ds} = \frac{\nabla n}{n}; \quad (4)$$

where s is the path distance. Our FPE ray theory comparisons used only the central path of a ray bundle. However, upon comparison of (3) and (4), a full-field theory effectively enhances the free-space operator to accommodate refraction. Figure 1 shows the optical path for a ray bundle launched from representative earth surface into a Chapman layer. Contours of constant optical path are phase fronts, which vary linearly in the propagation coordinate system, indicating beam steering. We review and demonstrate reconstruction of beam fields from ray optics.

References

[1] C. Rino and C. Carrano. A vector theory for forward propagation in a structured ionosphere. [illegible] 2021. doi.org/10.1016/j.jastp.2021.105558.

[2] C. Rino and C. Carrano. A vector theory for forward propagation in a structured ionosphere with a conducting boundary. [illegible] 223, 2021. doi.org/10.1016/j.jastp.2021.105740.

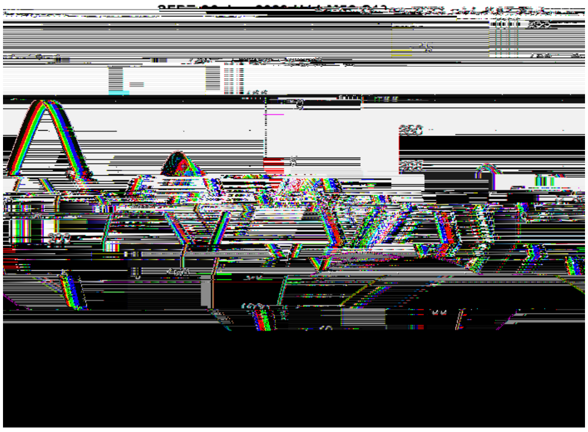

Figure 1. Display of 10 MHz optical path for a ray bundle launched from a curved earth surface into a Chapman layer.

[illegible]

Rino, Charles *[1], Charles Carrano[1], Matthew Proctor[1], Dima Paznukhov[1], and Keith Groves[1]

(1) Institute for Scientific Research, Boston College, Chesnut Hill, MA, USA

1 [illegible]

Beacon satellite signal processing for ionosphere diagnostics starts with sampled intensity and phase (GPS) or differential phase (dual-frequency systems). Scintillation is a complex modulation imparted to the signal. The signal phase includes a Doppler-shift contribution due to changing range and a contribution proportional to the path-integrated electron density (TEC). Dual-frequency measurements are used to remove the geometric-Doppler contribution. The residual TEC contribution is slowly varying. TEC measurement can be degraded by scintillation, which varies more rapidly. The low-frequency content of intensity scintillation is suppressed by Fresnel filtering. However, signal intensity varies inversely with path length and directionally varying antenna patterns. The scintillation index, $S_4 = \sqrt{\langle I^2\rangle / \langle I\rangle^2 - 1}$, is a standard measure of scintillation intensity, which is biased by additive noise. Preprocessing operations are used to isolate scintillation and TEC. Noise bias correction is also desirable under low signal-to-noise (SNR8 -0Pc35741 0 -32(correction)-y1>Tj /T1_1 9.963 Tf 38.498 0 Td (by)Tj /C0_2

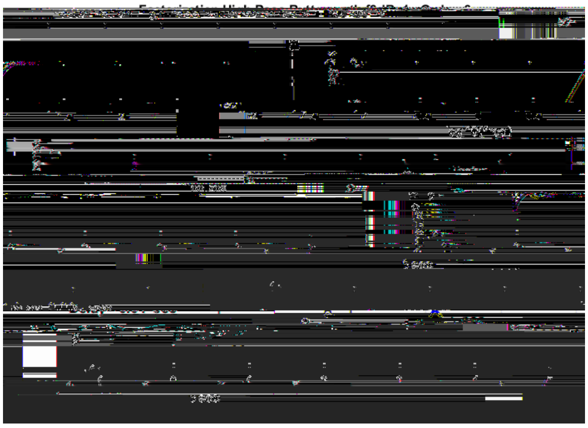

1 Top frame compares exact (blue) and toolbox (green) Butterworth lter. Middle frame shows transfer functions. Bottom frame shows step response for lter delay.

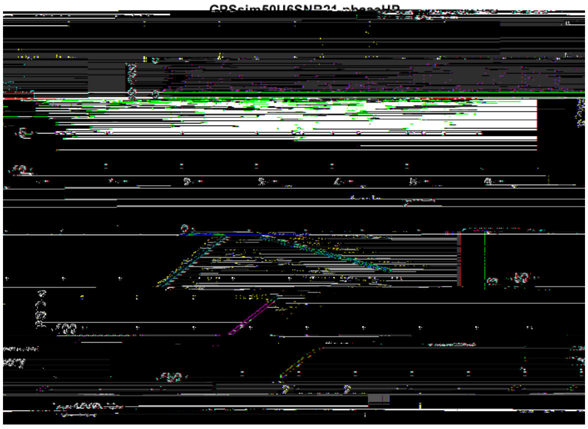

2 Top frame is ltered phase from simulated scintillation with $S_4 = 0.6$. Lower frame shows measured phase spectrum (blue) with de ning phase-screen spectrum. High frequency phase enhancement is due to phase jumps.

R

[DKH93] A. J. Van Dierendonck, J. Klobuchar, and Q. Hua. Ionospheric scintillation monitoring using commercial single frequency c/a code receivers. Proc. ION ITM, Salt Lake City, UT, (September), 1993.

[Rino1971] C. Rino. Factorization of Spectra by Discrete Fourier Transforms IEEE Transactions on Information Theory 1971 July 1970

Improving IRI's topside formulation for a better assimilation of GNSS TEC data during the local winter

Servan-

Reviving High-Speed Releases using Sounding Rockets and the Space Measurements of A Rocket-Released Turbulence (SMART) Experiment

Siefring, Carl US Naval Research Laboratory, Plasma Physic Division

Ganguli, Gurudas

Gatling, George

Coombs, Joseph

Crabtree, Christopher

Fletcher, Alex

Amatucci, William

Netwall, Christopher

Falcone, Nicholas (Naval Surface Warfare Center)

Ferrell, William (NASA Goddard Space Flight Center)

Holzworth, Robert (University of Washington)

McCarthy, Michael (University of Washington)

Space Measurements of A Rocket-Released Turbulence (SMART) is a sounding rocket
a1-ed.835.15d5]1(chol)-13.831 T755cou-5.1sne1Co[(a).9J 133d (s)Tj 0[3t 49248 Twud-(h7248 Twy459ir

lightning generated whistler waves) is of particular importance to the dynamics in the inner magnetosphere and the radiation belts, but also has more global relevance, e.g. in solar wind

The Development of the Radio Frequency Ionospheric Scintillation Attribution (RISA) Tool

Smith, Dallin AFRL

Ronald Caton[1], Keith Groves[2], Theodore Beach[2], Charles Carrano[2], Alan Hoskinson[2], William McNeil[2], Donald Mizuno[2]

[1]Air Force Research Laboratory, Ionospheric Impact Branch, Kirtland AFB, NM 87117

[2]Boston College, Institute for Scientific Research, Chestnut Hill, MA 02467

Scintillation occurs when radio waves traverse ionospheric plasma turbulence or irregularities and develop random fluctuations in amplitude, phase, and other signal properties. Scintillation negatively impacts systems with trans-ionospheric radio links such as satellite communications, PNT (position, navigation, and timing) systems and space-

Characterization of the Daytime Ionosphere with ICON EUVAirglow Limb Profiles

Stephan, Andrew

A "Prediction Model" for the Occurrence or No-occurrence of Density Irregularity in Space Constructed with the ROCSAT Data

Su, Shin-Yi *National Central University, Taiwan*

S.-Y. Su[1,2], H.-H. Ho[2,3], C.-K. Chao[1,2], L.-C. Tsai[1], and C. H. Liu[4]

1. Center for Space and Remote Sensing Research, National Central University, Chung-Li, Taiwan.

2. Department of Space Science and Engineering, National Central University, Chung-Li, Taiwan.

3. Central Weather Bureau, Taipei, Taiwan.

4. Academia Sinica, Taipei, Taiwan.

The density variations at a constant height such as observed by the circularly orbiting ROCSAT-1 spacecraft are studied to construct a "prediction model" for the occurrence or no-occurrence of an equatorial plasma bubble (EPB). This global prediction model is different from previous studies carried out at a local ground station by observing the variation of the ionospheric height and the occurrence of equatorial spread-F/EPB events. The model uses the density increment above the seasonal mean to predict the EPB occurrences. It does not merely provide the occurrence probability of EPB occurrences. Instead, the ROCSAT "prediction model" is to predict the occurrence or no-occurrence of the density irregularity/EPB along the ROCSAT orbit by constructing a contingency table to count the number of successes in predicting the EPB occurrences, failures in predicting the occurrences, and false alarms in a month. Different thresholds of density increment are used for the criteria in the prediction to obtain the optimal result in the prediction model. The optimal model for predicting the global irregularity/EPB occurrences varies between 75% and 85% for any season in 1999 to 2004.

Equatorial Irregularities

Estimation of Ionospheric Scintillation Index S4 from Rate of Change of Total Electron Content Index (ROTI) in Low Latitudes